# Shaft Trajectory Analysis in a Partially Demagnetized Permanent-Magnet Synchronous Motor

Julio-César Urresty, Reza Atashkhooei, Jordi-Roger Riba, *Member, IEEE*, Luís Romeral, *Member, IEEE*, and Santiago Royo

***Abstract*—Demagnetization faults have a negative impact on the behavior of permanent-magnet synchronous machines, thus reducing their efficiency, generating torque ripple, mechanical vibrations, and acoustic noise, among others. In this paper, the displacement of the shaft trajectory induced by demagnetization faults is studied. It is proved that such faults may increase considerably the amplitude of the rotor displacement. The direct measure of the shaft trajectory is performed by means of a noncontact self-mixing interferometric sensor. In addition, the new harmonics in the back electromotive force (EMF) and the stator current spectrum arising from the shaft displacement are analyzed by means of finite-element method (FEM) simulations and experimental tests. Since conventional finite-element electromagnetic models are unable to predict the harmonics arising from the shaft trajectory displacement, an improved finite-element model which takes into account the measured trajectory has been developed. It is shown that this improved model allows obtaining more accurate back EMF and stator current spectra than those obtained by means of conventional models. This work presents a comprehensive analysis of the effects generated by demagnetization faults, which may be useful to develop improved fault diagnosis schemes.**

***Index Terms*—Demagnetization, displacement measurement, fault diagnosis, finite-element methods (FEMs), harmonic analysis, lasers, optical interferometry, permanent-magnet machines.**

## NOMENCLATURE

| | |
|---|---|
| $f_{\text{demag}}$ | Demagnetization fault harmonic frequencies. |
| $f_e$ | Line frequency. |
| $k$ | Integer number (1, 2, 3, . . .). |
| $P$ | Number of pole pairs. |
| $Q$ | Number of slots in the stator. |
| $q$ | Number of slots per pole per phase. |
| $N$ | Number of turns in a slot. |
| $X$ | $X$-axis. |
| $Y$ | $Y$-axis. |

Manuscript received March 29, 2012; revised June 27, 2012; accepted August 8, 2012. Date of publication August 16, 2012; date of current version April 11, 2013. This work was supported in part by the Spanish Ministry of Science and Technology under the TRA2010-21598-C02-01, DPI2009-13379, and DPI2011-25525 research projects.

J.-C. Urresty and L. Romeral are with the Motion Control and Industrial Applications, Department of Electronic Engineering, Universitat Politècnica de Catalunya, 08222 Terrassa, Spain (e-mail: julio.urresty@mcia.upc.edu; romeral@eel.upc.edu).

R. Atashkhooei and S. Royo are with the Centre for Sensors, Instruments, and Systems Development (CD6), Universitat Politècnica de Catalunya, 08222 Terrassa, Spain (e-mail: reza.atashkhooei@cd6.upc.edu; santiago.royo@upc.edu).

J.-R. Riba is with the Department of Electric Engineering, Universitat Politècnica de Catalunya (UPC), 08034 Barcelona, Spain, and also with the Motion Control and Industrial Applications, Department of Electronic Engineering, UPC, 08222 Terrassa, Spain (e-mail: riba@ee.upc.edu).

Color versions of one or more of the figures in this paper are available online at http://ieeexplore.ieee.org.

Digital Object Identifier 10.1109/TIE.2012.2213565

## I. INTRODUCTION

PERMANENT-MAGNET synchronous machines (PMSMs) are currently being applied in a large type of demanding applications, such as servo actuators, robotics, aeronautical applications, or high-rise elevators and are a serious option for electric traction systems [1], [2]. Most of these applications require compactness, broad speed and torque range, and high efficiency. It is well known that PMSM technology offers highly attractive features, including high efficiency, precise torque control, high power density, and high torque-to-current ratio, among others [3], [4]. Improved efficiency is due in part because PMSMs do not present excitation copper losses since they do not have excitation windings [5].

Traditionally, fault diagnosis in electrical machines has been virtually limited to overvoltage and overcurrent protection. This system has the drawback of requiring bringing the machine offline once the fault has been detected [6]. However, in critical applications, this action mode may not be acceptable since a safe operation must be ensured [7]. Therefore, a more selective protection system is required to minimize unscheduled shutdowns. Hence, this selectivity requires developing a reliable fault diagnosis scheme which should be able to detect incipient failures. Among the methods developed in recent years, which include vibration [8] and thermal analysis, stator current analysis has been widely applied for incipient fault detection [9].

Demagnetization jointly with bearing and rotor eccentricity faults are the major sources of failures in PMSMs [10]. Eccentricity faults may be classified into static, dynamic, or mixed eccentricity. Such faults may generate excessive noise and vibration, unbalanced magnetic pull, and bearing damage [11]. Eccentricity faults may be originated by load unbalance and misalignment, a bent rotor shaft, or incorrect mounting [12]. Therefore, rotor faults are often classified into eccentricity failures and flux disturbances due to defects in the permanent magnets.

Motor current signature analysis (MCSA) is one of the most popular methods to diagnose electric motor faults because it does not disturb the normal motor operation, is noninvasive, and only requires a current sensor [13]. Since traditional MCSA-related methods are based on Fourier analysis, MCSA has some inherent limitations because it should be applied under stationary speed and load operating conditions. It is so because speed changes and load oscillations among other effects may distort the current spectra [13]. Despite these drawbacks, fault diagnosis methods based on signatures obtained from the fast Fourier transform line current spectra are still being analyzed [14]. In consequence, when the motor operates under

nonstationary conditions, other mathematical methods different from the classical Fourier analysis are applied, including time-frequency analysis [2], wavelet analysis [13], or Vold–Kalman filtering order tracking [15].

Demagnetization faults in PMSMs are troublesome [16] and may generate permanent motor performance and efficiency degradation [10]. Different phenomena such as high stator currents, interturn short circuits, significant temperature raise, or cracks in the magnets may lead to partial demagnetization of the rotor magnets. Partial demagnetization has adverse mechanical effects since it causes unbalanced magnetic pull, magnetic force harmonics, acoustic noise, and vibrations. Therefore, partial demagnetization reduces considerably the mechanical torque of the PMSM and severely affects motor performance [17], [18].

The effects of demagnetization faults have been studied extensively in the last few years [19], [20]. In [16], it was verified that demagnetization faults impact both the torque and the sound power emitted by the machine due to radial forces. Generation of vibrations and acoustic noise was studied in external rotor PMSM with nonoverlapping windings [21]. However, as far as we know, there are no studies concerning the link between demagnetization and mechanical effects such as deviations of the rotor trajectory. In this paper, it is proved that demagnetization faults in PMSMs lead unavoidably to the generation of unbalanced magnetic forces which, in turn, may generate a deviation of the rotor trajectory. The evidences presented in this study resulting from both finite-element method (FEM) simulations and the direct measurement of the 2-D motor shaft displacement in $X$- and $Y$-axes by means of self-mixing interferometry (SMI) using two laser diodes support this hypothesis. As it is well known, demagnetization faults in PMSMs induce fractional harmonics in the stator current spectrum. This work is focused to understand the origin of these fractional harmonics. To this end, a widened point of view is applied, which includes the analysis of the mechanical effects arising from demagnetization faults.

## II. Harmonic Components Due to Demagnetization Faults

It is well known that a healthy machine induces a regular and periodic back electromotive force (EMF) voltage in each slot of the stator windings [4]. Conversely, when dealing with a partially demagnetized machine, the back EMF induced in a single slot is not regular. It is so because the damaged magnets do not have the same contribution in the back EMF than the others, thus producing a gap or asymmetry in its waveform whenever a damaged magnet passes in front of a given slot. Since the back EMF losses its sinusoidal shape because of the partially demagnetized magnets, new harmonic components appear in the back EMF which may be transmitted to the stator currents depending on the stator winding configuration [4].

The harmonic content in the back EMF greatly influences the output torque ripple, noise emissions, and vibrations, thus deteriorating the behavior of the PMSM. Torque ripple in PMSMs should be minimized particularly in applications requiring speed and position accuracy [20].

In the technical literature, it is well documented that demagnetization faults induce the following set of harmonic frequencies in the stator current spectrum [12], [19], [22]:

$$f_{\text{demag}} = f_e \left(1 \pm \frac{k}{P}\right), \qquad k = 1, 2, 3, \ldots \tag{1}$$

$f_{\text{demag}}$ being the fault harmonic frequencies due to partial demagnetization, $f_e$ being the electrical supply frequency, and $P$ being the number of pole pairs of the machine. This chain of fault frequencies is present in both constant speed and nonstationary conditions. In this latter case, the fault harmonics change in frequency and amplitude, depending on the operational point of the motor. The harmonic components present in the stator current profiles may be used to design a noninvasive scheme to detect demagnetization faults.

Stator current diagnostic by means of monitoring and analyzing the stator current spectrum has been applied successfully to detect these types of faults [1], [19]. However, as stated in [22], depending on the stator winding configuration and the type of demagnetization, in some cases, no new harmonic or subharmonic frequencies that are different than those already present in a healthy machine appear due to demagnetization faults. Hence, in these cases, these faults must be detected by analyzing other machine variables. Additionally, it is also known that other types of rotor defects may be detected by studying the same characteristic fault frequencies in the stator currents as predicted by (1). For example, in [11], it is stated that mixed eccentricity faults lead to the chain of frequencies around the fundamental given by (1).

Rotor eccentricity distorts the air-gap flux distribution since the air-gap length has a notable influence on the flux path. In the region where the air-gap length diminishes, the magnetic flux may increase, and therefore, it may lead to saturation effects and motor performance reduction [23]. Similarly, eccentricity faults may also have a profound impact on the air-gap flux distribution. In the case of demagnetization faults, the air-gap flux distribution is also distorted when compared with that of a healthy machine [4].

As stated, demagnetization faults and other types of rotor defects may have a similar impact on the stator current spectra. Consequently, depending on the stator winding configuration, in some cases, it is difficult to distinguish between demagnetization and other types of rotor faults by analyzing the stator current spectrum.

In this paper, it is proved that a partially demagnetized PMSM generates unbalanced magnetic forces which may produce a deviation of the rotor trajectory. It is shown that these unbalanced forces are originated by the magnetic interaction between the ferromagnetic stator core and the rotor magnets. In addition, it is demonstrated that the trajectory deviation may produce visible changes in the stator current spectrum, which may be useful for fault diagnosis purposes.

## III. Magnetic Analysis of Demagnetization Faults

In this section, the effects of partial demagnetization faults are analyzed by means of 2-D FEM simulations using the

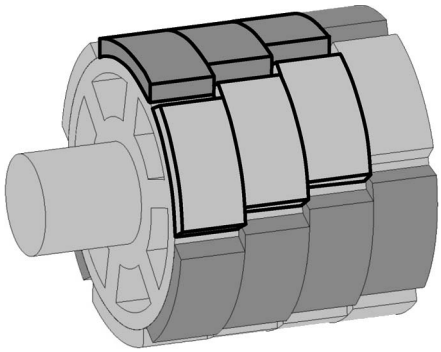

Fig. 1. Type of demagnetization analyzed in this work. The demagnetized magnets are dashed in solid black line. The rotor was mechanically balanced to avoid additional vibrations and orbital trajectories different from these induced by the analyzed effect.

commercial FLUX package and experimental results. Finite-element analysis has been widely applied for designing and analyzing electrical machines [24]. A FEM model of a healthy and a partially demagnetized surface-mounted permanent-magnet synchronous motor (SPMSM) taking into account the parameters shown in Table II (see the Appendix section) and the details shown in Fig. 1 was created for this purpose. To perform the FEM simulations, the motor is controlled by means of a closed-loop controller with an outer speed loop and two inner current loops ($i_d^* = 0$ and $i_q$).

The faulty SPMSM has two 75% partially demagnetized poles as shown in Fig. 1. To achieve this demagnetization pattern, six rotor magnets placed in consecutive poles were removed and demagnetized. Afterward, they were placed in their original position to facilitate the motor mechanical balancing. Next, to avoid abnormal vibration of the rotor and, consequently, anomalous orbital trajectories, the rotor mass was balanced.

Fig. 2 shows the results obtained by means of FEM simulations of the stator currents of both a healthy and a partially demagnetized machine. These simulations suppose the motor shaft rotating perfectly around its symmetry axis.

In [4], it is stated that integral slot windings tend to remove from the stator current spectrum the effects of periodic changes of parameters that may modify the magnetic flux. Results shown in Fig. 2 clearly show that the fractional harmonics predicted by (1) are not present in the simulated current spectrum. It is due to the particular winding configuration of the analyzed motor, an integral slot winding with $q = 1$ slots per pole per phase. Note that the main difference between both spectra (healthy and partially demagnetized motors) is that the amplitude of the odd harmonics is lower for the partially demagnetized motor.

To conduct the experimental validation, a healthy ABB 380-Vac SPMSM and a partially demagnetized ABB 380-Vac SPMSM driven by an ABB DGV-700 power converter are used. These motors have rated speed of 6000 r/min, rated current of 2.9 A, and present rotor skewing. During the experimental tests, both motors are loaded with an identical SPMSM that acts as a load, driven by its own power converter. Hence, the motors can be tested under different load conditions.

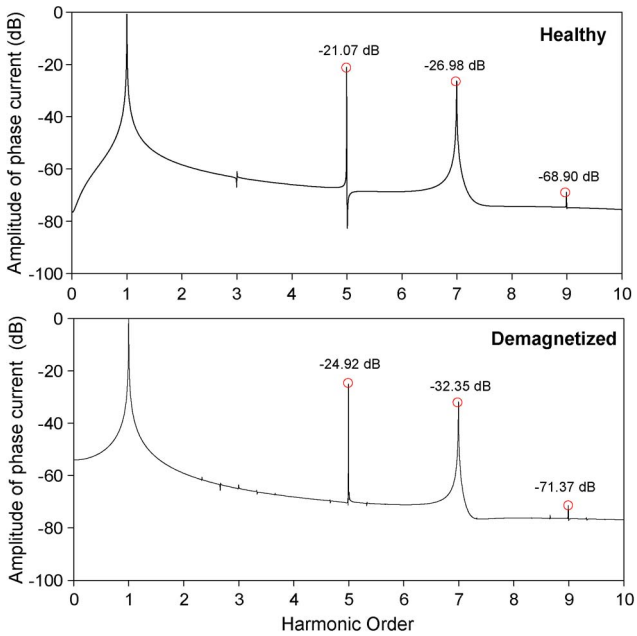


Fig. 2. Stator current spectra of a healthy and a partially demagnetized SPMSM operating at 1500 r/min under rated load. FEM simulation results.

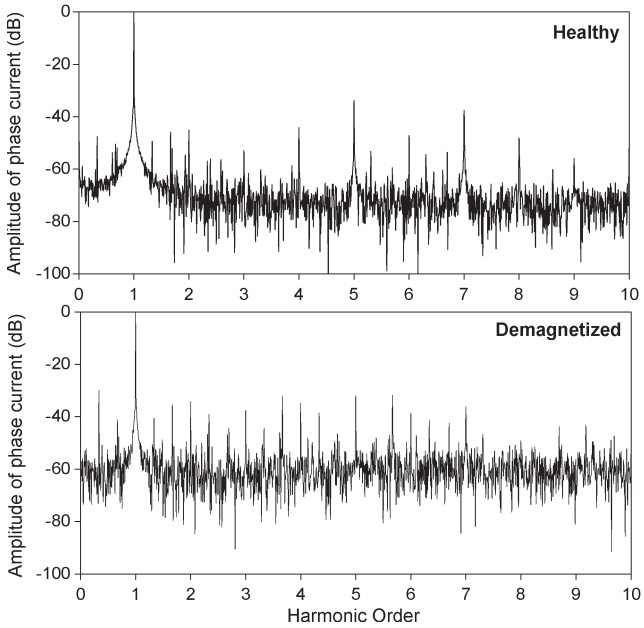


Fig. 3. Stator current spectra of a healthy and a partially demagnetized SPMSM operating at 1500 r/min under rated load. Experimental results.

Fig. 3 shows the spectra of the experimental currents, for both a healthy and a faulty SPMSM running at 1500 r/min under rated load.

Experimental spectra shown in Fig. 3 are more complex than those obtained from FEM simulations since the former show the presence of fractional and even harmonics for both healthy and partially demagnetized machines. FEM simulations suppose the SPMSM fed by ideal sources, whereas it is well known that the motor controller may inject harmonics [25]. Additionally, the fractional harmonics may be also due to mechanical causes such as inherent rotor misalignments and eccentricities [20].

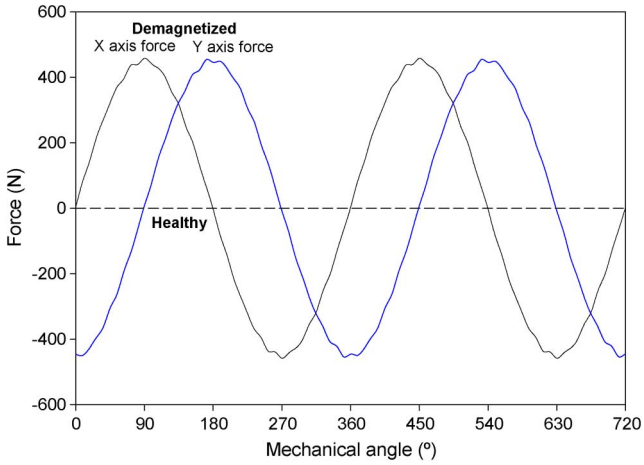


Fig. 4. Radial magnetic forces on the shaft of a healthy and a partially demagnetized SPMSM when operating at 1500 r/min under rated load. FEM simulation results.

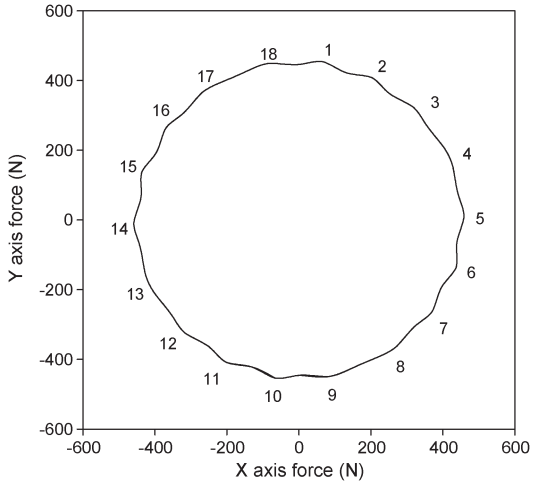


Fig. 5. $Y$-axis force against $X$-axis force for the partially demagnetized SPMSM operating at 1500 r/min under rated load. FEM simulation results.

To explain the presence of fractional harmonics, this study must be extended to analyze possible mechanical effects arising from demagnetization faults. It is well known that there is a magnetic attraction force between the ferromagnetic stator core and the rotor magnets. These radial forces may be obtained from FEM simulations, as shown in Fig. 4.

Simulation results from Fig. 4 show that, in the case of the healthy SPMSM, these radial forces are equilibrated. However, in the case of the partially demagnetized SPMSM, there is a nonzero resultant radial force which must generate mechanical effects.

Fig. 5 plots the $Y$-axis force against the $X$-axis force, which have been obtained from FEM simulations of the partially demagnetized SPMSM. It clearly shows 18 lobules corresponding to the $Q = 18$ stator slots.

The influence of the stator currents on the radial forces was analyzed. To this end, two simulations were performed. In the first one, the SPMSM was simulated when operating at rated load (rated current), while in the second, it was analyzed under no-load conditions, as shown in Fig. 6.

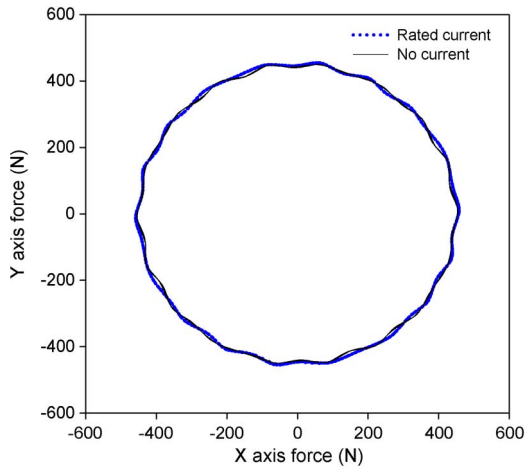


Fig. 6. $Y$-axis force against $X$-axis force for the partially demagnetized SPMSM operating at 1500 r/min under rated load and no-load conditions. FEM simulation results.

Results from Fig. 6 show that the stator currents have nearly no contribution to the resultant radial force. Consequently, it can be assumed that this force is only due to the magnetic interaction between the ferromagnetic stator core and the rotor magnets.

Although the analyzed SPMSM has wye-connected stator windings, a delta connection is expected to lead to similar magnetic forces since they are originated by the interaction between the rotor magnets and the ferromagnetic stator core. This also applies to other configurations, including parallel-connected coils.

## IV. Analysis of Mechanical Effects of Demagnetization Faults

In this section, the shaft trajectory of a healthy and a partially demagnetized SPMSM is measured experimentally. As deduced from Figs. 4–6, it seems feasible that the unbalanced magnetic forces present in a partially demagnetized machine may induce small displacements of the motor shaft. Therefore, to analyze in detail the effects of such forces, an exhaustive combined electromagnetic and mechanical FEM model of the machine that must include the behavior of the bearings is required. However, this is not an easy solution. Fortunately, the shaft displacement may be measured experimentally. In practice and in order not to affect the measurement, optimally, the shaft displacement should be observed using some noncontact measurement system. In this paper, the system has been measured using a double SMI setup, shown in Fig. 7. The setup contains two self-mixing laser diodes (SMLDs) and associate electronics placed perpendicular to each other pointing toward the rotating shaft, to sample its 2-D displacement along the $X$- and $Y$-axes.

SMI is an experimental technique which has been extensively used for displacement, vibration, and velocity sensing during the past decades [26]–[28]. It is based on measuring the beat arising from the interference of a portion of the laser beam back reflected into the laser cavity by a moving target (the motor shaft in this case) and the standing wave inside the cavity. Since the SMI configuration is compact, self-aligned, robust, and

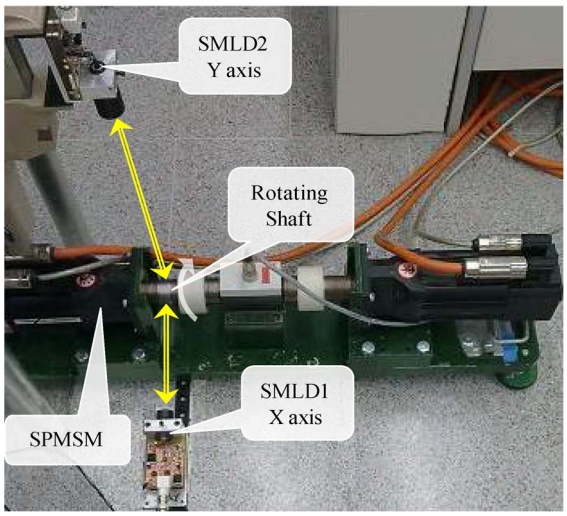


Fig. 7. Experimental setup used to measure the deviations in the shaft trajectory of the analyzed SPMSMs.

cheap in comparison with conventional interferometers, it is particularly attractive from the industrial application viewpoint.

As there are a number of different types of noise sources in the measuring environment, such as structural vibrations or shaft surface roughness and shape deviations, a low-pass filter is applied to the acquired self-mixing signal. Afterward, a transition detection algorithm [29] is used as the signal processing method, yielding a resolution of half the wavelength of the laser (392 nm) in the technique. The two orthogonal SMLDs' configuration allows direct measurements of the motor shaft displacement since the readings of both laser diodes were acquired simultaneously. Two Hitachi HL7851G Fabry–Pérot laser diodes with a maximum output power of 50 mW, emitting at the wavelength of 785 nm, were used in the experiment. The laser measuring system was not attached to the motor frame in order to avoid vibrations generated by the motor.

Hence, by comparing the measures obtained from a healthy and a partially demagnetized motor, the mechanical effects of the demagnetization faults become visible. Figs. 8 and 9 show the trajectories of the target point of the motor shaft where both laser beams were pointing to.

As proved in Figs. 8 and 9, both the healthy and faulty SPMSMs have a certain degree of eccentricity, but it becomes significantly higher in the latter. Therefore, these results are a consistent proof that demagnetization faults may increase significantly the amplitude of the shaft displacement. Concretely, results shown in Fig. 9 show a measured displacement of about $\pm 30$ $\mu$m ($\pm 5\%$ of the air gap) for the partially demagnetized SPMSM.

## V. Analysis of Joint Mechanical and Magnetic Effects of Demagnetization Faults

In Section IV, it has been shown that results from conventional FEM models of the SPMSM that do not include the shaft displacement are not in close agreement with experimental results. Therefore, in this section, the experimental displacement of the motor shaft is included in the FEM simulations. As it will be proved, this procedure allows performing more realistic

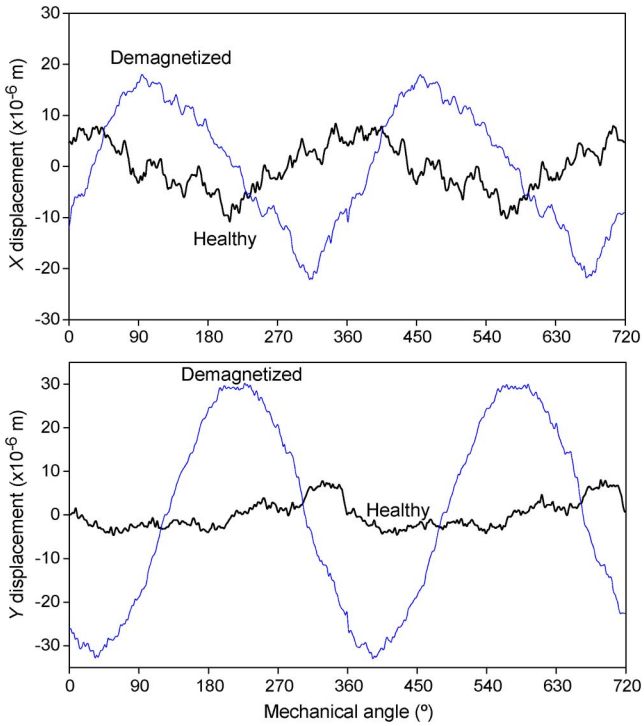


Fig. 8. Displacement of the motor shaft as measured by the two SMLDs placed in the $X$- and $Y$-axes. A healthy SPMSM and a partially demagnetized SPMSM were measured when running at 1500 r/min under no-load conditions.

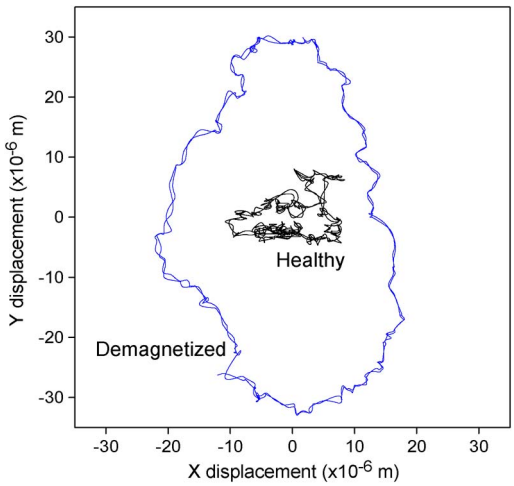


Fig. 9. Trajectory of the measured target point of the motor shaft in the $X$–$Y$ plane. A healthy SPMSM and a partially demagnetized SPMSM were measured when running at 1500 r/min under no-load conditions.

simulations since they take into account the shaft displacement, which is certainly present in real motors.

The experimental results shown in Figs. 8 and 9 for both healthy and partially demagnetized motors will be used to adjust the FEM model that takes into account the displacement of the motor shaft. It will allow explaining the mechanical effects due to demagnetization faults.

A healthy SPMSM presents an almost constant reluctance if neglecting the slot effects. Contrarily, when dealing with a partially demagnetized SPMSM, the reluctance changes with the rotor angular position. It is so because of the displacement of the motor shaft (air-gap variation) due to the radial forces.

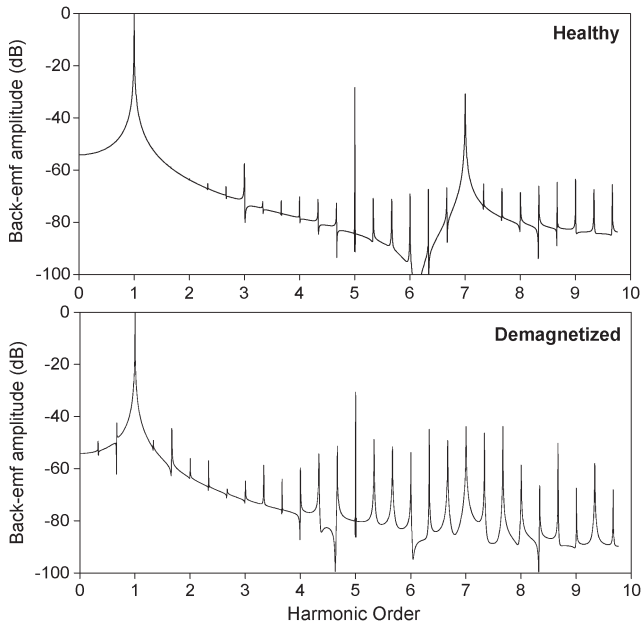


Fig. 10. Phase-to-phase back-EMF spectrum of a healthy and a partially demagnetized SPMSM operating at 1500 r/min under rated load. Simulation results obtained by introducing the measured displacements of the motor shaft in the FEM model.

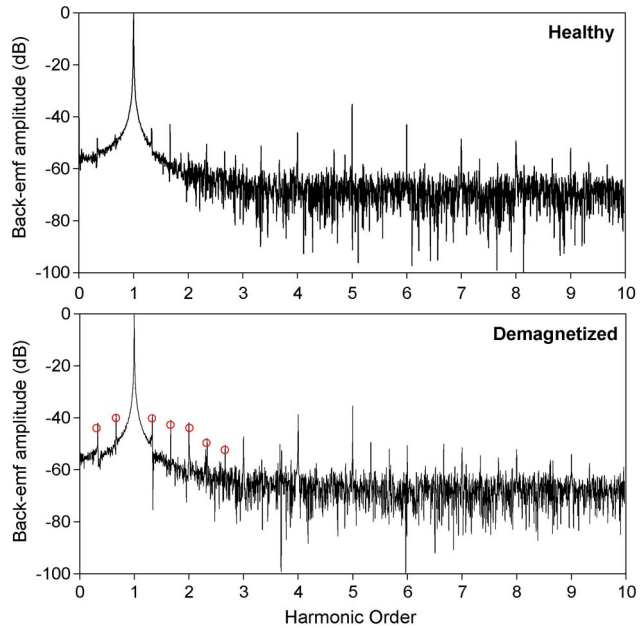


Fig. 11. Phase-to-phase back-EMF spectrum of a healthy and a partially demagnetized SPMSM operating at 1500 r/min under rated load. Experimental results.

Additionally, due to the shaft displacement, the magnetic flux due to the permanent magnets is also altered. Hence, these combined effects are traduced in stator flux variations, which are reflected and amplified (due to the time derivative) in the back-EMF spectrum, as shown in Fig. 10. Results from Fig. 10 show that, when considering a FEM model including both the effects of demagnetization and eccentricity, the back-EMF spectrum contains fractional harmonics. Back-EMF simulation results must be checked with experimental results, which are shown in Fig. 11.

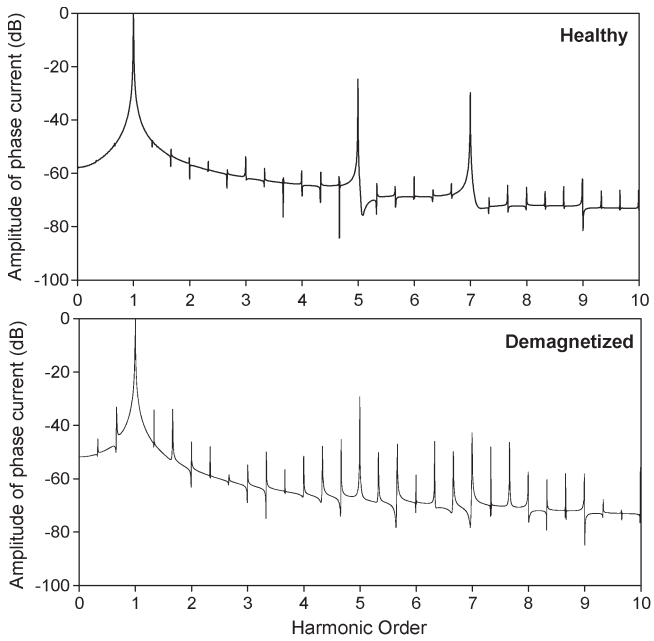


Fig. 12. Phase current spectrum of a healthy and a partially demagnetized SPMSM operating at 1500 r/min under rated load. Simulation results obtained by introducing the measured displacements of the motor shaft in the FEM model.

Although the experimental back-EMF spectra are more complex than the simulated ones, results from Fig. 11 clearly show that the back-EMF spectrum of the demagnetized SPMSM contains fractional harmonics as predicted by the simulations.

Fig. 12 shows the simulated spectrum of the stator current when taking into account the shaft displacement.

Results from Fig. 12 show the presence of fractional harmonics as in the experimental stator current spectra shown in Fig. 3. It should be pointed out that, when considering the demagnetization effects but not the shaft displacement (see Fig. 2), there is no presence of fractional harmonics in the stator current spectrum. Hence, these results show that demagnetization faults may amplify the amplitude of the shaft displacement already present in any healthy motor, which, in turn, may induce fractional harmonics in the current spectrum.

## VI. Conclusion

This work has analyzed the change in the shaft trajectory produced by partial demagnetization in SPMSMs. These faults are common in SPMSMs and may severely deteriorate the motor performance, thus leading to a premature ageing or an irreversible fault condition. Preliminary FEM simulations have shown that a demagnetized machine generates unbalanced radial forces which may generate mechanical effects. By means of two SMLDs, the shaft trajectories of a healthy and a partially demagnetized machine have been measured. This work has introduced this innovative sensor to measure the shaft displacement. The experimental data provided by the SMLDs clearly show that demagnetization faults may significantly increase the amplitude of the shaft displacement when compared with a healthy machine. To obtain more realistic results than those obtained by means of conventional electromagnetic FEM models, an improved FEM model that includes the measured shaft

TABLE I
STATOR WINDING CONNECTION DIAGRAM

| Slots | | | | | | | | | | | | | | | | | |
|---|---|---|---|---|---|---|---|---|---|---|---|---|---|---|---|---|---|
| 1 | 2 | 3 | 4 | 5 | 6 | 7 | 8 | 9 | 10 | 11 | 12 | 13 | 14 | 15 | 16 | 17 | 18 |
| Phases (A,B,C), coils (1,2,3) and direction of current (+,-) | | | | | | | | | | | | | | | | | |
| + | - | + | - | + | - | + | - | + | - | + | - | + | - | + | - | + | - |
| A1 | C1 | B1 | A1 | C1 | B1 | A2 | C2 | B2 | A2 | C2 | B2 | A3 | C3 | B3 | A3 | C3 | B3 |
| Magnets | | | | | | | | | | | | | | | | | |
| N | | | S | | | N | | | S | | | N | | | S | | |

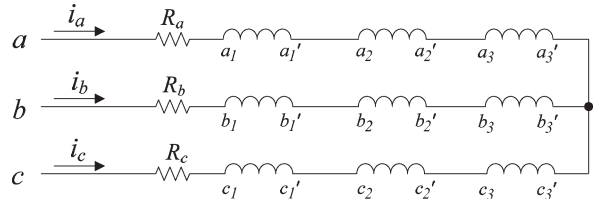


Fig. 13. Stator winding connections.

trajectory has been developed. Therefore, the proposed FEM model takes into account, in a straightforward and realistic manner, mechanical effects due to the bearing components, possible misalignments, or bending in the shaft, among others. It is worth noting that these effects are not included in conventional electromagnetic FEM models.

Therefore, these changes may be visible in stator current spectrum as fractional harmonics. In this paper, it has been proved that, as a consequence of the particular stator winding configuration (integral slot windings), these fractional harmonics are a consequence of the motor shaft displacement due to the unbalanced magnetic forces. It has been shown that the improved FEM model that includes the measured shaft displacement presents more realistic results than conventional FEM models. Therefore, the results of this work may be useful to develop improved fault diagnosis schemes and new fault indicators, since, as far as we know, the shaft trajectory displacement due to demagnetization faults has been taken into account for the first time.

The SPMSMs analyzed have integral slot windings. This type of windings tends to remove from the stator current spectrum the effects of periodic changes of parameters that may modify the magnetic flux. However, the particular demagnetization faults analyzed in this work generate an irregular trajectory of the motor shaft that makes visible the fractional fault harmonic frequencies in the stator current spectra.

## APPENDIX

Table I shows the winding configuration of the three-phase SPMSMs analyzed in this work.

Both the healthy and the partially demagnetized SPMSMs have symmetrical concentrated stator windings connected in series, six poles ($P = 3$), four magnets per pole (the rotor has six rows with four permanent magnets in each row), 144 turns per phase, 18 stator slots, and 48 turns per slot, which result in $q = 1$ slots per pole per phase.

Fig. 13 shows a diagram of the winding connections.

Table II shows additional parameters of the analyzed SPMSM. These parameters are used to generate the FEM model whose simulation results are exposed in the following sections.

TABLE II
GEOMETRIC PARAMETERS AND MATERIALS OF THE SPMSMS ANALYZED

| | |
|---|---|
| Manufacturer | ABB |
| Converter model | DGV 700 |
| Rated voltage | 380 Vac |
| Rated current | 2.9 A |
| Rated torque | 2.3 Nm |
| Rated speed | 6000 r/min |
| Poles pairs | 3 |
| Stator slots | 18 |
| Stator slots per phase | 6 |
| Stator windings connection type | wye |
| $N$ | 144 turns/phase |
| $R_s$ | 1.50 Ω (1.1% unbalance) |
| $L$ | 4.9 mH |
| $M$ | -0.90 mH |
| Magnets type | NdFeB |
| Magnets per pole | 4 |
| Magnets remanent magnetic flux density | 1.18 T |
| Stator steel saturation magnetic flux density | 1.8 T |
| Axial length | 89 mm |
| Stator outer radius | 40.49 mm |
| Air gap | 0.6 mm |
| Rotor outer radius | 22.8 mm |
| Magnets height | 2.5 mm |
| Shaft radius | 9 mm |

## REFERENCES

[1] S. Rajagopalan, W. Roux, T. G. Habetler, and R. G. Harley, "Dynamic eccentricity and demagnetized rotor magnet detection in trapezoidal flux (brushless DC) motors operating under different load conditions," *IEEE Trans. Power Electron.*, vol. 22, no. 5, pp. 2061–2069, Sep. 2007.

[2] J.-R. Riba, A. Garcia, and L. Romeral, "Demagnetization diagnosis in permanent magnet synchronous motors under non-stationary speed conditions," *Elect. Power Syst. Res.*, vol. 80, no. 10, pp. 1277–1285, Oct. 2010.

[3] L. Romeral, J.-C. Urresty, J.-R. Riba, and A. Garcia, "Modeling of surface-mounted permanent magnet synchronous motors with stator winding interturn faults," *IEEE Trans. Ind. Electron.*, vol. 58, no. 5, pp. 1576–1585, May 2011.

[4] J.-C. Urresty, J.-R. Riba, M. Delgado, and L. Romeral, "Detection of demagnetization faults in surface-mounted permanent magnet synchronous motors by means of the zero-sequence voltage component," *IEEE Trans. Energy Convers.*, vol. 27, no. 1, pp. 42–51, Mar. 2012.

[5] K. I. Laskaris and A. G. Kladas, "Permanent-magnet shape optimization effects on synchronous motor performance," *IEEE Trans. Ind. Electron.*, vol. 58, no. 9, pp. 3776–3783, Sep. 2011.

[6] A. Gandhi, T. Corrigan, and L. Parsa, "Recent advances in modeling and online detection of stator interturn faults in electrical motors," *IEEE Trans. Ind. Electron.*, vol. 58, no. 5, pp. 1564–1575, May 2011.

[7] M. Delgado, A. Garcia, J.-R. Riba, J.-C. Urresty, and J. A. Ortega, "Feature extraction of demagnetization faults in permanent-magnet synchronous motors based on box-counting fractal dimension," *IEEE Trans. Ind. Electron.*, vol. 58, no. 5, pp. 1594–1605, May 2011.

[8] B. M. Ebrahimi and J. Faiz, "Magnetic field and vibration monitoring in permanent magnet synchronous motors under eccentricity fault," *IET Elect. Power Appl.*, vol. 6, no. 1, pp. 35–45, Jan. 2012.

[9] B. Akin, S. Choi, U. Orguner, and H. A. Toliyat, "A simple real-time fault signature monitoring tool for motor-drive-embedded fault diagnosis systems," *IEEE Trans. Ind. Electron.*, vol. 58, no. 5, pp. 1990–2001, May 2011.

[10] J. Hong, S. Park, D. Hyun, T. Kang, S. B. Lee, C. Kral, and A. Haumer, "Detection and classification of rotor demagnetization and eccentricity faults for PM synchronous motors," *IEEE Trans. Ind. Appl.*, vol. 48, no. 3, pp. 923–932, May/Jun. 2012.

[11] S. Nandi, T. C. Ilamparithi, S. B. Lee, and D. Hyun, "Detection of eccentricity faults in induction machines based on nameplate parameters," *IEEE Trans. Ind. Electron.*, vol. 58, no. 5, pp. 1673–1683, May 2011.

[12] W. le Roux, R. G. Harley, and T. G. Habetler, "Detecting rotor faults in low power permanent magnet synchronous machines," *IEEE Trans. Power Electron.*, vol. 22, no. 1, pp. 322–328, Jan. 2007.

[13] M. Pineda-Sanchez, M. Riera-Guasp, J. Roger-Folch, J. A. Antonino-Daviu, J. Perez-Cruz, and R. Puche-Panadero, "Diagnosis of induction motor faults in time-varying conditions using the polynomial-phase transform of the current," *IEEE Trans. Ind. Electron.*, vol. 58, no. 4, pp. 1428–1439, Apr. 2011.
[14] S. Choi, B. Akin, M. M. Rahimian, and H. A. Toliyat, "Performance-oriented electric motors diagnostics in modern energy conversion systems," *IEEE Trans. Ind. Electron.*, vol. 59, no. 2, pp. 1266–1277, Feb. 2012.
[15] J.-C. Urresty, J.-R. Riba, and L. Romeral, "Diagnosis of inter-turn faults in PMSMs operating under non-stationary conditions by applying order tracking filtering," *IEEE Trans. Power Electron.*, vol. 28, no. 1, pp. 507–515, Jan. 2013.
[16] D. Torregrossa, A. Khoobroo, B. Fahimi, F. Peyraut, and A. Miraoui, "Prediction of acoustic noise and torque pulsation in PM synchronous machines with static eccentricity and partial demagnetization using field reconstruction method," *IEEE Trans. Ind. Electron.*, vol. 52, no. 2, pp. 934–944, Feb. 2012.
[17] K. C. Kim, S. B. Lim, D. H. Koo, and J. Lee, "The shape design of permanent magnet for permanent magnet synchronous motor considering partial demagnetization," *IEEE Trans. Magn.*, vol. 42, no. 10, pp. 3485–3487, Oct. 2006.
[18] S. Ruoho, J. Kolehmainen, J. Ikaheimo, and A. Arkkio, "Interdependence of demagnetization, loading, temperature rise in a permanent-magnet synchronous motor," *IEEE Trans. Magn*, vol. 46, no. 3, pp. 949–953, Mar. 2010.
[19] J.-R. Riba, J. A. Rosero, A. Garcia, and L. Romeral, "Detection of demagnetization faults in permanent-magnet synchronous motors under nonstationary conditions," *IEEE Trans. Magn.*, vol. 45, no. 7, pp. 2961–2969, Jul. 2009.
[20] J. C. Urresty, J. R. Riba, L. Romeral, and A. Garcia, "A simple 2-D finite-element geometry for analyzing surface-mounted synchronous machines with skewed rotor magnets," *IEEE Trans. Magn.*, vol. 46, no. 11, pp. 3948–3954, Nov. 2010.
[21] J. Krotsch and B. Piepenbreier, "Radial forces in external rotor permanent magnet synchronous motors with non-overlapping windings," *IEEE Trans. Ind. Electron*, vol. 59, no. 5, pp. 2267–2276, May 2012.
[22] D. Casadei, F. Filippetti, C. Rossi, and A. Stefani, "Magnets faults characterization for permanent magnet synchronous motors," in *Proc. IEEE SDEMPED*, 2009, pp. 1–6, 2009.
[23] S. M. Mirimani, A. Vahedi, and F. Marignetti, "Effect of inclined static eccentricity fault in single stator–single rotoraxial flux permanent magnet machines," *IEEE Trans. Magn.*, vol. 48, no. 1, pp. 143–149, Jan. 2012.
[24] G. Y. Sizov, D. M. Ionel, and N. A. O. Demerdash, "Modeling and parametric design of permanent-magnet AC machines using computationally efficient finite-element analysis," *IEEE Trans. Ind. Electron.*, vol. 59, no. 6, pp. 2403–2413, Jun. 2012.
[25] W. Le Roux, R. G. Harley, and T. G. Habetler, "Detecting faults in rotors of PM drives," *IEEE Ind. Appl. Mag.*, vol. 14, no. 2, pp. 23–31, Mar./Apr. 2008.
[26] S. Ottonelli, M. Dabbicco, F. de Lucia, M. di Vietro, and G. Scamarcio, "Laser self mixing interferometry for mechatronics applications," *Sensors*, vol. 9, no. 5, pp. 3527–3548, May 2009.
[27] M. Norgia, A. Magnani, and A. Pesatori, "High resolution self-mixing laser rangefinder," *Rev. Sci. Instrum.*, vol. 83, no. 4, pp. 045113-1–045113-6, Apr. 2012.
[28] U. Zabit, R. Atashkhooei, T. Bosch, S. Royo, F. Bony, and A. D. Rakic, "Adaptive self-mixing vibrometer based on a liquid lens," *Opt. Lett.*, vol. 35, no. 8, pp. 1278–1280, Apr. 2010.
[29] C. Bes, G. Plantier, and T. Bosch, "Displacement measurements using a self-mixing laser diode under moderate feedback," *IEEE Trans. Instrum. Meas.*, vol. 55, no. 4, pp. 1101–1105, Aug. 2006.

**Julio-César Urresty** received the M.S. degree in electrical engineering and the M.S. degree in physics from the Universidad del Valle, Cali, Colombia, in 2006 and 2009, respectively. He is currently working toward the Ph.D. degree in the Motion Control and Industrial Applications, Department of Electronic Engineering, Universitat Politècnica de Catalunya, Terrassa, Spain.

His research interests include signal processing methods, electric machines, variable-speed drive systems, and fault detection algorithms.

**Reza Atashkhooei** was born in Khoy, Iran, in 1977. He received the M.Sc. degree in photonics from the Universitat Politècnica de Catalunya (UPC), Barcelona, Spain, in 2008. He is currently working toward the Ph.D. degree in optical engineering in the Centre for Sensors, Instruments, and Systems Development (CD6), UPC, Terrassa, Spain.

His current research interests include vibration and velocity measurements for industrial applications, signal processing, adaptive optics, and optical metrology.

**Jordi-Roger Riba** (M'09) received the M.S. degree in physics and the Ph.D. degree from the Universitat de Barcelona, Barcelona, Spain, in 1990 and 2000, respectively.

He is with the Universitat Politècnica de Catalunya (UPC), Barcelona, Spain, where he joined the Escola d'Enginyeria d'Igualada as a full-time Lecturer in 1992 and the Department of Electric Engineering in 2001. He is also with the Motion Control and Industrial Applications, Department of Electronic Engineering, UPC, Terrassa, Spain. His research interests include electromagnetic device modeling, signal processing methods, electric machines, fault diagnosis in electric machines, and fault detection algorithms.

**Luís Romeral** (M'98) received the M.S. degree in electrical engineering and the Ph.D. degree from the Universitat Politècnica de Catalunya (UPC), Barcelona, Spain, in 1985 and 1995, respectively.

In 1988, he joined the Department of Electronic Engineering, UPC, Terrassa, Spain, where he is currently an Associate Professor and the Director of the Motion Control and Industrial Applications, whose major research activities concern induction and permanent-magnet motor drives, enhanced efficiency drives, fault detection and diagnosis of electrical motor drives, and improvement of educational tools. He has developed and taught postgraduate courses on programmable logic controllers, electrical drives and motion control, and sensors and actuators.

Dr. Romeral is a member of the European Power Electronics and Drives Association and the International Federation of Automatic Control.

**Santiago Royo** received the M.Sc. degree in physics from the Universitat de Barcelona, Barcelona, Spain, in 1992 and the Ph.D. degree in applied optics from the Universitat Politècnica de Catalunya (UPC), Barcelona, Spain, in 1999.

He is currently an Associate Professor with UPC, Terrassa, Spain, where he is the Director of the Centre for Sensors, Instruments, and Systems Development (CD6), a research and innovation center in optical engineering with staff of 40 people, and leads projects involving adaptive optics, 3-D imaging, and optical metrology, specializing in wavefront sensing and self-mixing interferometry. He is also a Cofounder of one spin-off company of CD6, SnellOptics. His research interests involve adaptive optics, optical metrology, optical design and fabrication, and photometric testing.